



Transient response of stochastic finite element systems using Dynamic Variability Response Functions



Vissarion Papadopoulos*, Odysseas Kokkinos

Institute of Structural Analysis & Seismic Research, National Technical University of Athens, 9 Iroon Polytechniou, Zografou Campus, Athens 15780, Greece

ARTICLE INFO

Article history:

Received 17 February 2014
Received in revised form 29 September 2014
Accepted 30 September 2014
Available online 23 October 2014

Keywords:

Dynamic Variability Response Functions
Stochastic finite element analysis
Upper bounds
Stochastic dynamic systems

ABSTRACT

In this study a methodology is presented for effective analysis of dynamic systems with stochastic material properties. The concept of dynamic mean and variability response functions, recently established for linear stochastic single degree of freedom oscillators, is extended to general finite element systems such as statically indeterminate beam/frame structures and plane stress problems, leading to closed form integral expressions for their dynamic mean and variability response. The integrand of these integral expressions involves the spectral density function of the uncertain material properties and the so called dynamic mean and variability response functions respectively, which are assumed to be deterministic, i.e. independent of the power spectrum as well as the marginal *pdf* of the uncertain parameters. A finite element method-based fast Monte Carlo simulation procedure is used for the accurate and efficient numerical evaluation of these functions. In order to demonstrate the validity of the proposed procedure, the results obtained using the aforementioned integral expressions are compared to brute-force Monte Carlo simulation. As a further validation of the assumption of independence of the variability response function to the stochastic parameters of the problem, the concept of the generalized variability response function was applied and compared to the steady state dynamic variability response function. The methodology is applied in a dynamically loaded statically indeterminate beam/frame structure and a plane stress problem. The dynamic mean and variability response functions, once established, can be used to perform sensitivity/parametric analyses with respect to various probabilistic characteristics involved in the problem (i.e., correlation distance, standard deviation) and to establish realizable upper bounds on the dynamic mean and variance of the response, at practically no additional computational cost.

© 2014 Elsevier Ltd. All rights reserved.

1. Introduction

In recent years, multiple methodologies based on perturbation/expansion [1,2], spectral Galerkin approximations [3] or costly Monte Carlo methods [1,4–6] have been developed to deal with random/uncertain phenomena in steady state stochastic structural analysis and extended to dynamic stochastic analysis in a straightforward manner [7,8], along with procedures to improve their efficiency both in terms of accuracy [9–12] as well as computational performance [13–15]. A probability density evolution method was proposed in [16,17] in an effort to approximate the time varying probability distribution function (*pdf*) of the response of stochastic systems using the principle of preservation of probability. Along these lines, some other approaches implement approximate Wiener path integral solution schemes [18]. However these

approaches have been mainly implemented in single degree of freedom oscillators or small illustrative academic systems due to increased computational cost. In all above cases, prior knowledge of the correlation properties and the marginal *pdf* of the random fields characterizing system uncertainties is essential for accurate estimates of the system's response. In the frequent case of insufficient experimental data, analysts are forced to resort to sensitivity/parametric yet cost inefficient analyses. Furthermore, such analyses do not provide any information on the mechanisms that affect response variability, or bounds of the response. In addition to the aforementioned approaches, a relatively small number of studies have dealt with the dynamic propagation of system uncertainties, most of them reducing the stochastic dynamic PDE's to a linear random eigenvalue problem [19,20].

In order to effectively resolve aforementioned issues, a proposition has been made through the concept of Dynamic Variability Response Function (*DVRF*) in [21], which was a straightforward generalization of the currently classical *VRF* proposed in the late 1980s [22] along with different aspects and extensions [23,24].

* Corresponding author.

E-mail addresses: vpapado@central.ntua.gr (V. Papadopoulos), okokki@central.ntua.gr (O. Kokkinos).

DVRF involves information regarding deterministic variables of the problem and the standard deviation of the field modeling the random system parameters. In that work, closed form integral expressions involving DVRF and the spectral density function of the stochastic field, were suggested for the computation of the dynamic variance of the response displacement as follows:

$$\text{Var}[u(t)] = \int_{-\infty}^{\infty} \text{DVRF}(t, \kappa, \sigma_{ff}) S_{ff}(\kappa) d\kappa \quad (1)$$

An additional expression involving a Dynamic Mean Response Function (DMRF) for the system dynamic mean response was also proposed in that work. This approach was formulated for linear statically determinate single degree of freedom stochastic oscillators under dynamic excitations where it was demonstrated that the integral form expressions for the dynamic mean and variance can be used to effectively compute the first and second order statistics of the transient system response with reasonable accuracy, together with time dependent spectral-distribution-free upper bounds. They also provide an insight into the mechanisms controlling the uncertainty propagation with respect to both space and time and in particular the mean and variability time histories of the stochastic system dynamic response. Furthermore, once the DMRF and DVRF are established, sensitivity analyses with respect to various probabilistic parameters such as correlation distances and standard deviation were performed at a very small additional computational cost.

Based on the aforementioned recent development, closed form integral expressions in the form of Eq. (1) are proposed in the present work for the mean and variance of the dynamic response of statically indeterminate beam/frame structures and then extended to more general stochastic finite element systems (i.e. plane stress problems) under dynamic excitations. In this case DVRF and DMRF are vectors comprised of a DMRF and DVRF for each degree of freedom of the FE system. A general so-called Dynamic FEM fast Monte Carlo simulation (DFEM-FMCS) is provided for the accurate and efficient evaluation of DVRF and DMRF for stochastic FE systems. Numerical results are presented, demonstrating that, as in the case of classical VRFs, as well as in the case of DMRF and DVRF for single degree of freedom stochastic oscillators [21], the DVRF and DMRF matrices appear to be independent of the functional form of the power spectral density function $S_{ff}(\kappa)$ and appear to be marginally dependent on the pdf of the field modeling the uncertain system parameter. It is reminded that the existence of VRF has been proven only in the case of statically determinate structures under static loading [22,25]. In all other cases this existence had to be conjectured and the validity of this conjecture was demonstrated through comparisons of the results obtained from Eq. (1) with brute force MCS. The validity of this conjecture is further boosted in this work by comparing steady state DVRF with respective Generalized VRF [26] for a statically indeterminate frame structure. GVRF involves the computation of different VRFs for corresponding combinations of different marginal pdfs and power spectra and was developed in order to further test the validity of the existence of a VRF which is almost independent of the stochastic parameters of the problem. It should be mentioned here that the VRF concept was recently extended in [29] for structures with non-linear material properties where a closed form analytic expression of VRF revealed the clear dependence of the integral form of Eq. (1) on the standard deviation as well as higher order Power spectra of $f(x)$. Finally, realizable upper bounds of the mean and dynamic system response are evaluated.

2. Time-history analysis of stochastic finite element systems

Without loss of generality consider the linear stochastic FE system of Fig. 1 which is a fixed-fixed beam/frame structure. The

inverse of the elastic modulus is assumed to vary randomly along its length according to the following expression:

$$\frac{1}{E(x)} = F_0(1 + f(x)), \quad (2)$$

where E is the elastic modulus, F_0 is the mean value of the inverse of E , and $f(x)$ is a zero-mean homogeneous stochastic field modeling the variation of $1/E$ around its mean value.

For the derivation of the deterministic system dynamic response the trivial second-order differential equation for the discretized FE dynamic system equilibrium is as follows:

$$\mathbf{M}\ddot{\mathbf{u}}(t) + \mathbf{C}\dot{\mathbf{u}}(t) + \mathbf{K}\mathbf{u}(t) = \mathbf{P}(t) \quad (3)$$

where \mathbf{M} is the mass matrix of the discretized FE system, \mathbf{C} is its damping matrix, \mathbf{K} is its stiffness matrix and $\mathbf{P}(t)$ is its loading vector. At last, $\mathbf{u}(t)$ is the time-history of the displacement vector of the system, providing information about the response of each node of the FE mesh, $\dot{\mathbf{u}}(t)$ is the first order time-derivative and $\ddot{\mathbf{u}}(t)$ is the second order time-derivative of $\mathbf{u}(t)$.

Direct integration of Eq. (3) can be performed using i.e. a Newmark scheme of the following form:

$${}^{t+\Delta t}\hat{\mathbf{R}} = {}^{t+\Delta t}\mathbf{R} + \mathbf{M}(a_0{}^t\mathbf{U} + a_1{}^t\dot{\mathbf{U}} + a_2{}^t\ddot{\mathbf{U}}) + \mathbf{C}(a_1{}^t\mathbf{U} + a_4{}^t\dot{\mathbf{U}} + a_5{}^t\ddot{\mathbf{U}}) \quad (4)$$

where $a_0 = \frac{1}{a\Delta t^2}$; $a_1 = \frac{1}{a\Delta t}$; $a_2 = \frac{1}{2a} - 1$; $a_4 = \Delta t(1 - \delta)$; $a_5 = \delta\Delta t$; $a_6 = \Delta t(1 - \delta)$; $a_7 = \Delta t$. After choosing a time step Δt parameters α and δ are selected under the limitations $\delta \geq 0.50$ and $a \geq 0.25(0.5 + \delta)^2$. After initialization of ${}^0\mathbf{U}$, ${}^0\dot{\mathbf{U}}$, and ${}^0\ddot{\mathbf{U}}$, the displacements at time $t + \Delta t$ are calculated solving the following linear system of equations

$$\hat{\mathbf{K}}{}^{t+\Delta t}\mathbf{U} = {}^{t+\Delta t}\hat{\mathbf{R}} \quad (5)$$

where $\hat{\mathbf{K}}$ is the effective stiffness matrix given by

$$\hat{\mathbf{K}} = \mathbf{K} + a_0\mathbf{M} + a_1\mathbf{C} \quad (6)$$

Finally accelerations and velocities at time $t + \Delta t$ accrue from the following equations:

$${}^{t+\Delta t}\ddot{\mathbf{U}} = a_0({}^{t+\Delta t}\mathbf{U} - {}^t\mathbf{U}) - a_1{}^t\dot{\mathbf{U}} - a_2{}^t\ddot{\mathbf{U}} \quad (7)$$

$${}^{t+\Delta t}\dot{\mathbf{U}} = {}^t\dot{\mathbf{U}} + a_6{}^t\ddot{\mathbf{U}} + a_7{}^{t+\Delta t}\ddot{\mathbf{U}} \quad (8)$$

Matrices $\hat{\mathbf{R}}$ and $\hat{\mathbf{K}}$ in Eqs. (5) and (6) and consequently vectors \mathbf{U} , $\dot{\mathbf{U}}$ and $\ddot{\mathbf{U}}$ are random due to the variation of $E(x)$ in Eq. (2). Thus, the solution of Eq. (5) requires the implementation of some stochastic methodology in order to invert the stochastic operator $\hat{\mathbf{K}}$ in at each time step and predict the stochastic dynamic response of the FE system.

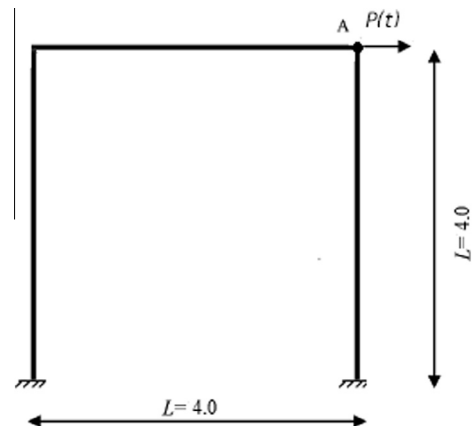


Fig. 1. Geometry and loading of the fixed-fixed frame discretized with 60 beam elements.

3. Analysis of mean and variance of dynamic system response using DMRF and DVRF

Following a procedure similar to the one presented in [21] for linear stochastic oscillators under dynamic loading, it is possible to express the variance of the dynamic response of a stochastic finite element system in the following integral form expression:

$$\text{Var}[\mathbf{u}(t)] = \int_{-\infty}^{\infty} \mathbf{DVRF}(t, \kappa, \sigma_{ff}) S_{ff}(\kappa) d\kappa \quad (9a)$$

where **DVRF** is the vectorized dynamic version of *DVRF*, assumed to be a function of deterministic parameters of the problem related to geometry, loading, (mean) material properties and the standard deviation σ_{ff} of the stochastic field modeling the system's flexibility. A similar integral expression can provide an estimate for the mean value of the dynamic response of the system [28]:

$$\varepsilon[\mathbf{u}(t)] = \int_{-\infty}^{\infty} \mathbf{DMRF}(t, \kappa, \sigma_{ff}) S_{ff}(\kappa) d\kappa \quad (9b)$$

where again **DMRF** is the vectorized dynamic version of *DMRF* of dimension equal to the dof's of the problem, which is a function similar to the **DVRF** in the sense that it also depends on deterministic parameters of the problem as well as σ_{ff} .

It is reminded here that the existence of Eqs. (9a) and (9b) has only been proved for statically determinate beams in which the resulting displacement field is a linear transformation of the stochastic field of the compliance $1/E(x)$ [25]. In all other cases this transformation is non linear. As demonstrated in [27], for such non linear transformations the integral expressions for the variance involve higher order spectra. Thus the nature of the approximation induced in Eqs. (9a) and (9b) is the omission of these higher order spectra.

3.1. Numerical estimation of the DVRF and the DMRF using fast Monte Carlo simulation

The numerical estimation of DVRF and DMRF involves a dynamic FEM-based fast Monte Carlo simulation (DFEM-FMCS) whose idea is to consider the random field $f(x)$ in Eq. (2) as a random sinusoid [28,29] and plug its monochromatic power spectrum into Eqs. (9a) and (9b), in order to compute the respective mean and variance response at various wave numbers as a function of time t . The steps of the FEM-FMCS approach are the following:

- (i) Generate N (5–10) sample functions of the below random sinusoid with standard deviation σ_{ff} and wave number $\bar{\kappa}$ modeling the variation of the inverse of the elastic modulus $1/E$ around its mean F_0 :

$$f_j(x) = \sqrt{2}\sigma_{ff} \cos(\bar{\kappa}x + \varphi_j) \quad (10)$$

where $j = 1, 2, \dots, N$ and φ_j varies randomly under uniform distribution in the range $[0, 2\pi]$. These samples are generated by dividing the range $[0, 2\pi]$ at 5–10 equally spaced distances and selecting the centres of these distances as values of random phase angles φ_j 's.

- (ii) Using these N generated sample functions it is straightforward to compute their respective dynamic mean and response variance, $\varepsilon[\mathbf{u}(t)]_{\bar{\kappa}}$ and $\text{Var}[\mathbf{u}(t)]_{\bar{\kappa}}$, by solving the corresponding FEM system under the applied dynamic loading using Eqs. (5), (7) and (8). Random matrix $\bar{\mathbf{K}}$ is constructed by assigning a different value of E at each FE, using i.e. the mid-point method.
- (iii) The value of the DMRF at wave number $\bar{\kappa}$ can then be computed as follows:

$$\mathbf{DMRF}(t, \bar{\kappa}, \sigma_{ff}) = \frac{\varepsilon[\mathbf{u}(t)]_{\bar{\kappa}}}{\sigma_{ff}^2} \quad (11a)$$

and likewise the value of the **DVRF** at wave number $\bar{\kappa}$

$$\mathbf{DVRF}(t, \bar{\kappa}, \sigma_{ff}) = \frac{\text{Var}[\mathbf{u}(t)]_{\bar{\kappa}}}{\sigma_{ff}^2} \quad (11b)$$

Both previous equations are direct consequences of the integral expressions in Eqs. (9a) and (9b) in the case that the stochastic field becomes a random sinusoid.

- (iv) Get **DMRF** and **DVRF** as a function of both time t and wave number κ by repeating previous steps for various wave numbers and different time steps. The entire procedure can be repeated for different values of the standard deviation σ_{ff} of the random sinusoid.

3.2. Bounds of the mean and variance of the dynamic response

Upper bounds on the mean and variance of the dynamic response of the stochastic system can be established directly from Eqs. (9a) and (9b), as follows:

$$\varepsilon[\mathbf{u}(t)] = \int_{-\infty}^{\infty} \mathbf{DMRF}(t, \kappa, \sigma_{ff}) S_{ff}(\kappa) d\kappa \leq \mathbf{DMRF}(t, \kappa^{\max}(t), \sigma_{ff}) \sigma_{ff}^2 \quad (12a)$$

$$\text{Var}[\mathbf{u}(t)] = \int_{-\infty}^{\infty} \mathbf{DVRF}(t, \kappa, \sigma_{ff}) S_{ff}(\kappa) d\kappa \leq \mathbf{DVRF}(t, \kappa^{\max}(t), \sigma_{ff}) \sigma_{ff}^2 \quad (12b)$$

where $\kappa^{\max}(t)$ is the wave number at which **DMRF** and **DVRF**, corresponding to a given time step t and value of σ_{ff} , reach their maximum value. For the minimum, $\kappa^{\max}(t)$ is substituted with $\kappa^{\min}(t)$ and inequality signs switch direction. An envelope of time evolving upper and lower bounds on the mean and variance of the dynamic system response can be extracted from Eqs. (12a) and (12b). As in the case of linear stochastic systems under static loads [27–29], this envelope is physically realizable since the form of the stochastic field that produces it is the random sinusoid of Eq. (10) with $\bar{\kappa} = \kappa^{\max}(t)$.

4. 2D formulation

In the case of a problem where the inverse elastic modulus is considered to vary randomly over a 2D domain, the following equation is adopted:

$$\frac{1}{E(x, y)} = F_0(1 + f(x, y)), \quad (13)$$

where E is the elastic modulus, F_0 is the mean value of the inverse of E , and $f(x, y)$ is now a two-dimensional, zero-mean homogeneous stochastic field modeling the variation of $1/E$ around its mean value F_0 . Accordingly, the integral expressions for the variance and mean response displacement $u(t)$ become:

$$\text{Var}[\mathbf{u}(t)] = \int_{-\infty}^{\infty} \int_{-\infty}^{\infty} \mathbf{DVRF}(t, \kappa_x, \kappa_y, \sigma_{ff}) S_{ff}(\kappa_x, \kappa_y) d\kappa_x d\kappa_y \quad (14a)$$

$$\varepsilon[\mathbf{u}(t)] = \int_{-\infty}^{\infty} \int_{-\infty}^{\infty} \mathbf{DMRF}(t, \kappa_x, \kappa_y, \sigma_{ff}) S_{ff}(\kappa_x, \kappa_y) d\kappa_x d\kappa_y \quad (14b)$$

where **DVRF**($t, \kappa_x, \kappa_y, \sigma_{ff}$) and **DMRF**($t, \kappa_x, \kappa_y, \sigma_{ff}$) are in this case two-dimensional, possessing the following bi-quadrant symmetries:

$$\mathbf{DMRF}(\kappa_x, \kappa_y) = \mathbf{DMRF}(-\kappa_x, -\kappa_y) \quad (15)$$

$$\mathbf{DVRF}(\kappa_x, \kappa_y) = \mathbf{DVRF}(-\kappa_x, -\kappa_y) \quad (16)$$

$S_{ff}(\kappa_x, \kappa_y)$ is the spectral density function of the stochastic field $f(x, y)$ possessing the same symmetries as **DMRF** and **DVRF**. The 1D random sinusoid in Eq. (10) now becomes a 2D one with the following form that is the same for all possible stochastic fields:

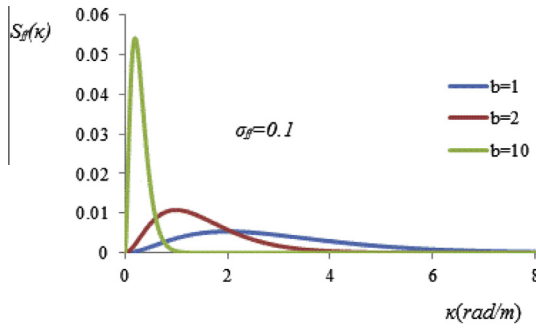


Fig. 2. Spectral density functions for stochastic field $f(x)$ standard deviation $\sigma_{ff} = 0.2$ for three different values of the correlation length parameter.

$$f_j(x) = \sqrt{2}\sigma_{ff} \cos(\bar{\kappa}_x x + \bar{\kappa}_y y + \varphi_j); \quad j = 1, 2, \dots, N. \quad (17)$$

Upper bounds on the mean and variance of the response displacement for a given time instance t can be established for the 2D case as follows:

$$\text{Var}[\mathbf{u}(t)] \leq \mathbf{DVRF}(t, \kappa_x^{\max}, \kappa_y^{\max}, \sigma_{ff}) \sigma_{ff}^2 \quad (18a)$$

$$\varepsilon[\mathbf{u}(t)] \leq \mathbf{DMRF}(t, \kappa_x^{\max}, \kappa_y^{\max}, \sigma_{ff}) \sigma_{ff}^2 \quad (18b)$$

where $(\kappa_x^{\max}, \kappa_y^{\max})$ is the wave number pair at which the **DMRF** or the **DVRF** take their maximum value (for a given value of σ_{ff} and a given location (x, y)), and σ_{ff}^2 is the variance of the stochastic field $f(x, y)$ modeling the inverse of the elastic modulus. Again, for the minimum, $\kappa_{x,y}^{\max}(t)$ is substituted with $\kappa_{x,y}^{\min}(t)$ and inequality signs switch direction. It should be emphasized that $(\kappa_x^{\max}, \kappa_y^{\max})$ are not necessarily the same for the **DMRF** and the **DVRF**.

5. GVRF formulation for static loading case

As mentioned previously, **DMRF** and **DVRF** conceptually are based on the assumption that they are deterministic, i.e. they are independent of the power spectral density type as well as of the marginal *pdf* used to describe the uncertain parameter of the problem. The validity of this conjecture is numerically demonstrated in the numerical examples by direct comparisons of the variance time history of the system response, computed with the proposed **DVRF**-based approach, with corresponding brute-force Monte Carlo simulations. As a further step of this validation, the recently established concept of **GVRF** [26] was utilized. For this purpose a **GVRF** for corresponding static loading cases was calculated for a family of moving **SDFs** and under a lognormal assumption for the modulus of elasticity and then compared to the **DVRF** computed via **DFEM-FMCS**.

5.1. GVRF estimation methodology

For a certain linear statically indeterminate structure with uncertain material properties, system variance response can be estimated by the following formula [22]

$$\text{Var}[u(x)] = \int_{-\infty}^{\infty} \text{VRF}(x, \kappa) S_{ff}(\kappa) d\kappa \quad (19)$$

where $\text{Var}[u(x)]$ can be readily computed by a brute-force Monte Carlo simulation. Eq. (19) can be rewritten in the following discretized form

$$\text{Var}[u(x)] = 2[S_f(\kappa_1) \quad S_f(\kappa_2) \quad \dots \quad S_f(\kappa_N)] \times \begin{bmatrix} \text{VRF}(x, \kappa_1) \\ \text{VRF}(x, \kappa_2) \\ \vdots \\ \text{VRF}(x, \kappa_N) \end{bmatrix} \Delta\kappa \quad (20)$$

Having assumed that **VRF** is independent of the power spectral density and the marginal *pdf*, it is natural to assume that the same **VRF** values can be used to estimate system variance for various **SDFs**. Therefore the following relation should also be true, only now that **VRF** is named **Generalized Variability Response Function (GVRF)**

$$\begin{bmatrix} \text{Var}[u(x)_1] \\ \text{Var}[u(x)_2] \\ \vdots \\ \text{Var}[u(x)_N] \end{bmatrix} = 2 \begin{bmatrix} S_{f_1}(\kappa_1) & S_{f_1}(\kappa_2) & \dots & S_{f_1}(\kappa_N) \\ S_{f_2}(\kappa_1) & S_{f_2}(\kappa_2) & \dots & S_{f_2}(\kappa_N) \\ \vdots & \vdots & \ddots & \vdots \\ S_{f_N}(\kappa_1) & S_{f_N}(\kappa_2) & \dots & S_{f_N}(\kappa_N) \end{bmatrix} \times \begin{bmatrix} \text{GVRF}(x, \kappa_1) \\ \text{GVRF}(x, \kappa_2) \\ \vdots \\ \text{GVRF}(x, \kappa_N) \end{bmatrix} \Delta\kappa \quad (21)$$

The left hand side vector is the vector of different system variances, calculated by respective brute-force Monte Carlo simulations, and the matrix on the right hand side is the matrix of **SDF** values for various corresponding spectral density types $S_{f_i}(\kappa), i = 1, 2, \dots, N$. Effectively, Eq. (21) describes a system of N linear equations with N unknowns, thus providing a unique solution for the **GVRF** vector.

6. Numerical examples

Example 1 For the fixed-fixed frame shown in Fig. 1 with length and height equal to $L = 4$ m, the inverse of the modulus of elasticity is assumed to vary randomly along its length according to Eq. (2) with $F_0 = (1.35 \times 10^8 \text{ kN/m})^{-1}$, $I = 0.1 \text{ m}^4$ and damping ratio $\xi = 5\%$. The total mass of the beam is assumed to be $m_{\text{tot}} = 6000$ kg, distributed evenly among the finite element nodes of the model. For the analysis of the frame structure we used 60 beam elements, 20 for each column and the plateau, of equal length, resulting in 177 d.o.f.'s.

Two load cases are considered: **LC1** consisting of a concentrated dynamic periodic load $P(t) = 100\sin(2t)$ at the right top corner of the frame (see Fig. 1) and **LC2** consisting of a dynamic load $p_n(t) = -m_n \ddot{U}_g(t)$ acting on each node n of the beam with m_n being the corresponding nodal mass and $\ddot{U}_g(t)$ the acceleration time history of the 1940 El Centro earthquake. The stochastic field $f(x)$ in Eq. (2) is considered to vary across the length of the two columns and the plateau of the frame running continuously from the left fixed edge to the right. The spectral density function (**SDF**) of Fig. 2 was used for the modeling of the inverse of the elastic modulus stochastic field, given by:

$$S_{ff}(\kappa) = \frac{1}{4} \sigma_{ff}^2 b^3 \kappa^2 e^{-b|\kappa|} \quad (22)$$

with $b = 1, 2, 10$ being three different values of the correlation length parameter examined.

For standard deviations σ_{ff} of the stochastic field $f(x)$ higher than 0.2 a truncated Gaussian and a lognormal *pdf* is used to model $f(x)$. For this purpose, an underlying Gaussian stochastic field denoted by $g(x)$ is generated using the spectral representation method [30] and the power spectrum of Eq. (22). The truncated Gaussian field $f_{\text{TC}}(x)$ is obtained by simply truncating $g(x)$ in the following way: $-0.9 \leq g(x) \leq 0.9$, while the lognormal $f_L(x)$ is obtained from the following transformation as a translation field [31]:

$$f_L(x) = F_L^{-1}\{G[g(x)]\} \quad (23)$$

The **SDF** of the underlying Gaussian field in Eq. (23) and the corresponding spectral densities of the truncated Gaussian and the Lognormal fields denoted $S_{f_{\text{TC}}}(\kappa)$ and $S_{f_L}(\kappa)$, respectively, are different from the one in Eq. (22) and are computed from the following formula

$$S_{f_{f_i}}(\kappa) = \frac{1}{2\pi L_x} \left| \int_0^{L_x} f_i(x) e^{-i\kappa x} dx \right|^2; \quad i = \text{TG, L} \quad (24)$$

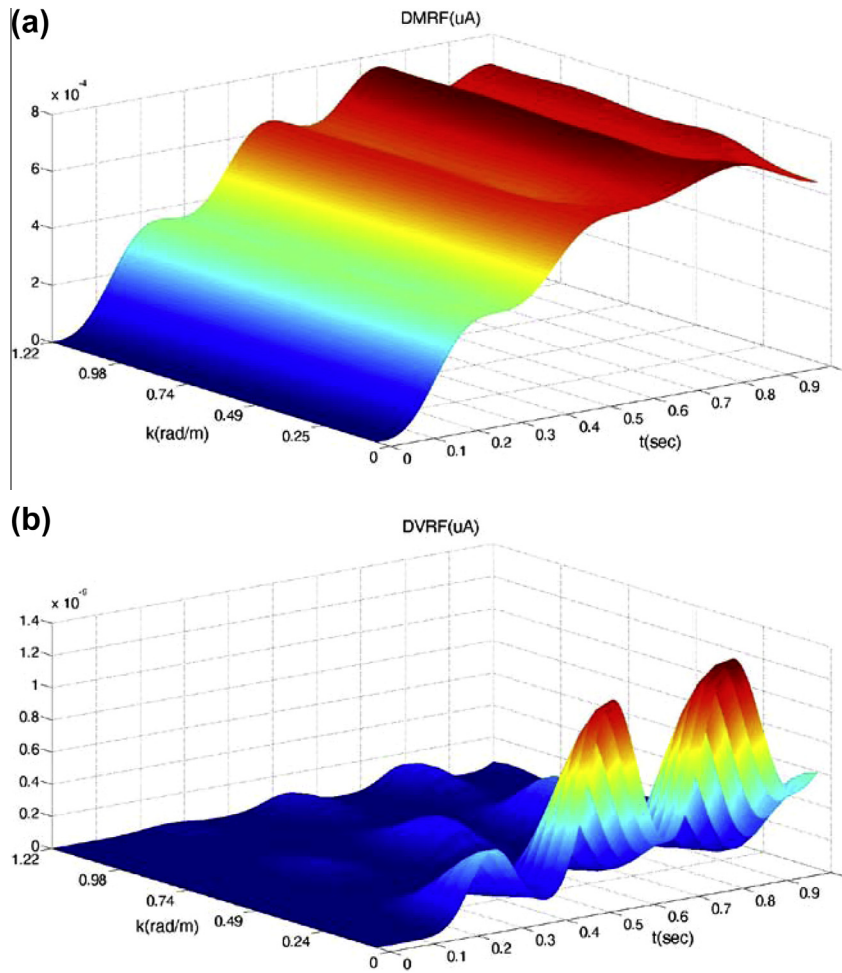


Fig. 3. 3D plots of (a) $DMRF$ and (b) $DVRF$ of the horizontal displacement u_A , as a function of frequency κ (rad/m) and time t (s) for LC1 and $\sigma_{ff} = 0.2$.

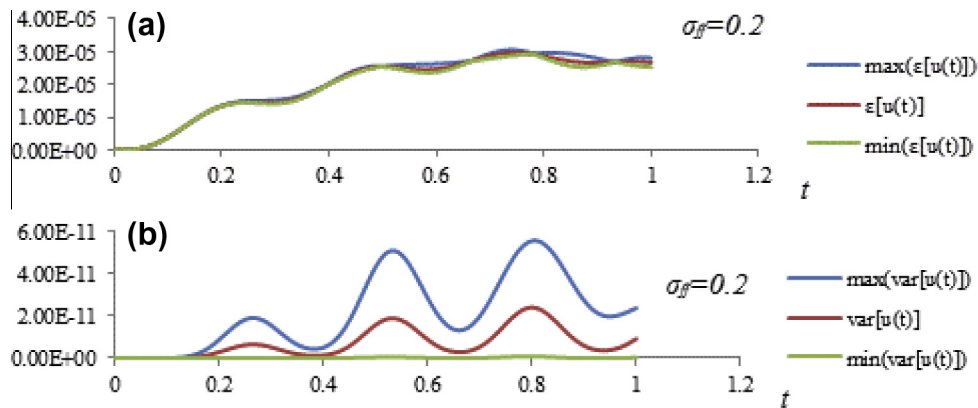


Fig. 4. Upper and lower bounds on the (a) mean and (b) variance of the response displacement for LC1 and $\sigma_{ff} = 0.2$.

where L_x is the length of the sample functions of the non-Gaussian fields modeling flexibility. As the sample functions of the non-Gaussian fields are non-ergodic, the estimation of power spectra in Eq. (24) is performed in an ensemble average sense [31].

Fig. 3 presents 3D plots of $DMRF(u_A)$ and $DVRF(u_A)$ for the horizontal displacement u_A of point A of the frame as a function of time t and frequency κ for $\sigma_{ff} = 0.2$. In this figure it can be observed that $DMRF(u_A)$ remains almost constant with respect to κ , while evol-

ing substantially as a function of t . On the contrary $DVRF(u_A)$ demonstrates a substantial volatility with respect to both κ and t . Therefore, in contrast to $DMRF(u_A)$, $DVRF(u_A)$ accommodates the possibility of considerable variation of the variability response for different statistical parameters of the stochastic field. This is further demonstrated in Fig. 4 in which the upper and lower bounds of the dynamic mean and variability response are depicted containing minima and maxima respectively, in comparison to the

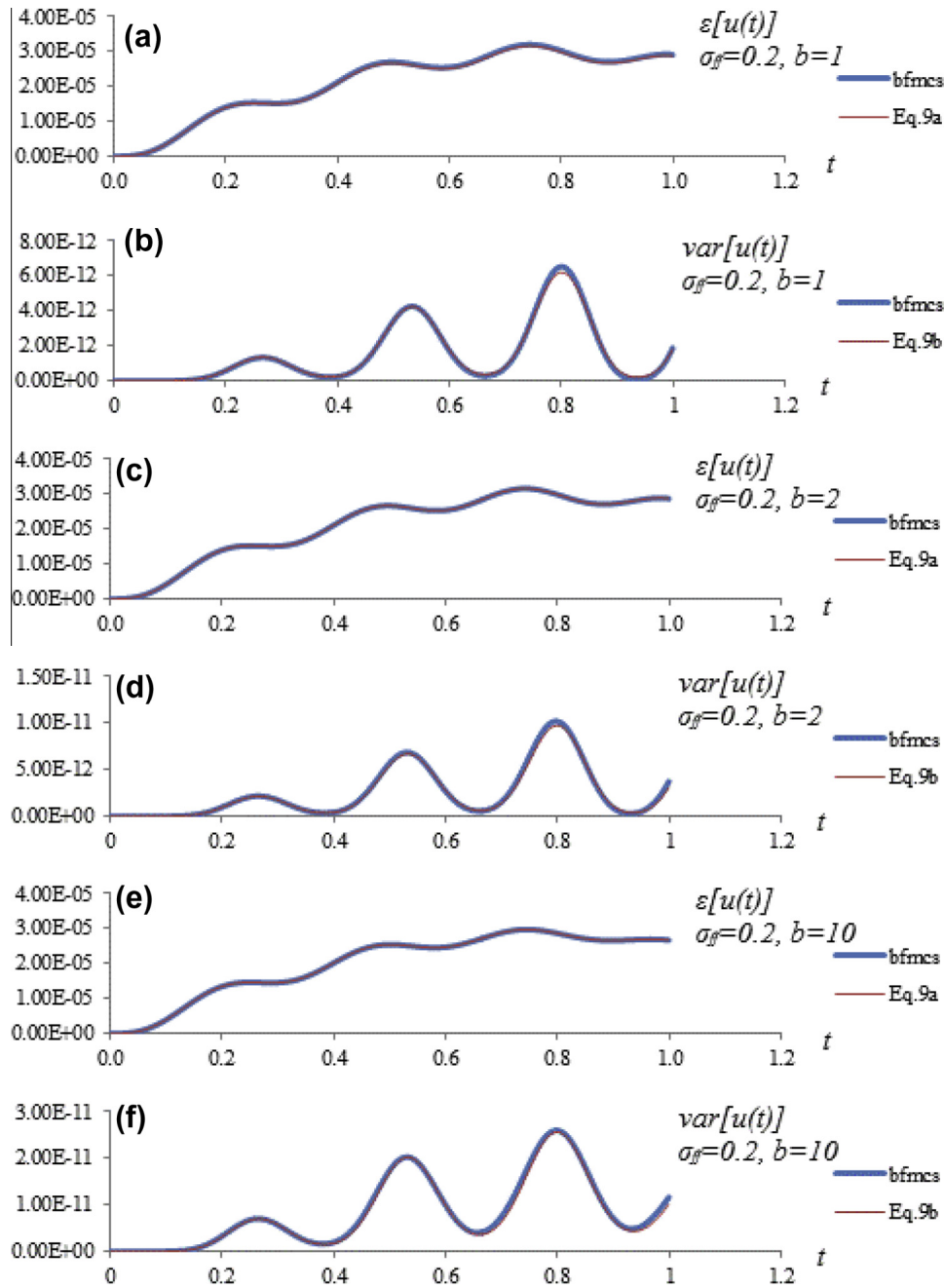


Fig. 5. Time histories of the (a), (c), (e) mean and (b), (d), (f) variance response displacement of the frame structure for a Gaussian field with $\sigma_{ff} = 0.2$ for LC1 and for three different correlation length parameter values $b = 1, 2$ and 10 . Comparison of results obtained from Eqs. (9a) and (9b) and MCS.

estimated mean and variability responses for the case of an underlying Gaussian stochastic field with the power spectrum of Eq. (22) and $\sigma_{ff} = 0.2$. The aforementioned bounds are derived directly from Eq. (12) having previously computed $DMRF(u_A)$ and $DVRF(u_A)$ with the computationally efficient DFEM-FMCS in Eq. (11), while in the case of the Gaussian field with $\sigma_{ff} = 0.2$, the mean and variance were obtained with the integral expression in Eq. (9). From this figure it can be seen that the upper mean dynamic response and the one estimated for the Gaussian field, are almost identical, while they differ significantly in the case of the response variability, reaching a maximum difference of more than 70% at $t = 0.8$ s. It should be pointed out here that bounds of each response do not necessarily need to coincide in the frequency number that they occur.

In order to demonstrate the validity of the proposed approach, the results obtained from the DFEM-FMCS procedure and Eq. (9) were compared with Brute Force Monte Carlo Simulation. In Fig. 5a–f the results of this comparison are presented for the dynamic mean and response variability of u_A (Fig. 2) and LC1, using a Gaussian stochastic field and $\sigma_{ff} = 0.2$, for three different values of correlation length parameter b . In this manner the independence of **DMRF** and **DVRF** from the spectral density function is also showcased. Figs. 6 and 7 present the same comparison but for a truncated Gaussian field with $\sigma_{ff} = 0.3912$ and 0.5286 , respectively, while Fig. 8 examines a lognormal field case with $\sigma_{ff} = 0.399$. Finally, Fig. 9 presents the same comparison but for the El Centro earthquake load case (LC2) and a Gaussian field with $\sigma_{ff} = 0.2$. From all these figures it can be observed that the results of the

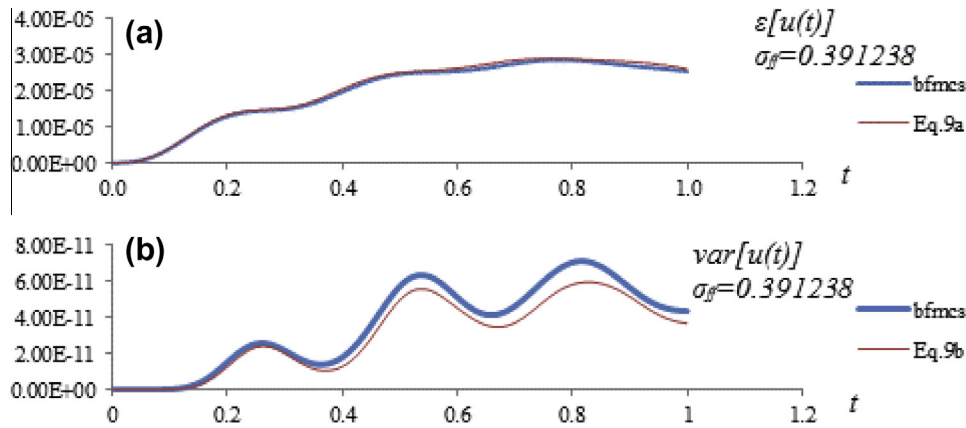


Fig. 6. Time histories of the (a) mean and (b) variance response displacement of the frame structure for a truncated Gaussian field with $\sigma_{ff} = 0.391238$ for LC1. Comparison of results obtained from Eqs. (9a) and (9b) and MCS.

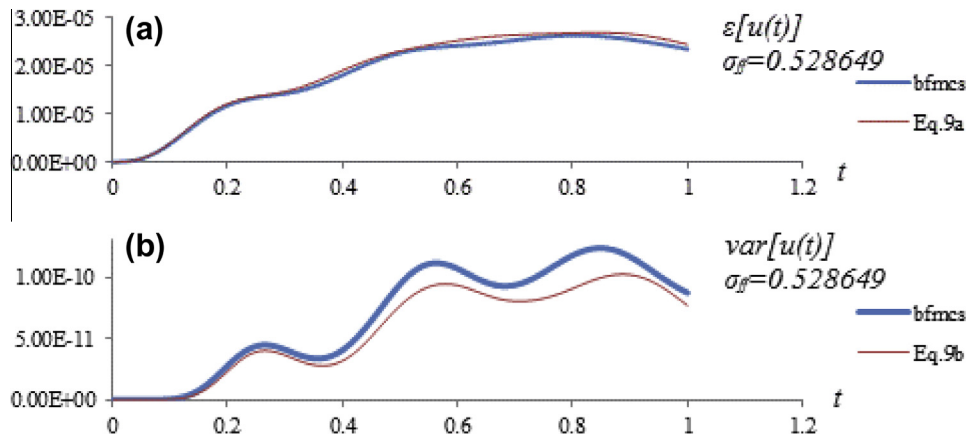


Fig. 7. Time histories of the (a) mean and (b) variance response displacement of the frame structure for a truncated Gaussian field with $\sigma_{ff} = 0.528649$ for LC1. Comparison of results obtained from Eq. (9a) and (9b) and MCS.

DFEM-FMCS are in close agreement with the corresponding results of MCS. The prediction of the mean value is almost identical for the two methods in all cases considered, while the maximum error in the variance does not exceed 20% and is attributed to a slight dependence of the DVRF on the pdf of the random field modeling $1/E(x)$. This error becomes negligible in the case of small standard deviations of the order of $\sigma_{ff} = 0.2$.

6.1. Further validation using GVRF

In Fig. 10 we demonstrate the convergence of the steady state DVRF(u_A) of the fixed-fixed frame to the GVRF(u_A) derived for the respective static solution for a truncated Gaussian and a Log-normal field of standard deviation $\sigma_{ff} = 0.1$. For this procedure a parent SDF S_p of exponential form has been used given by

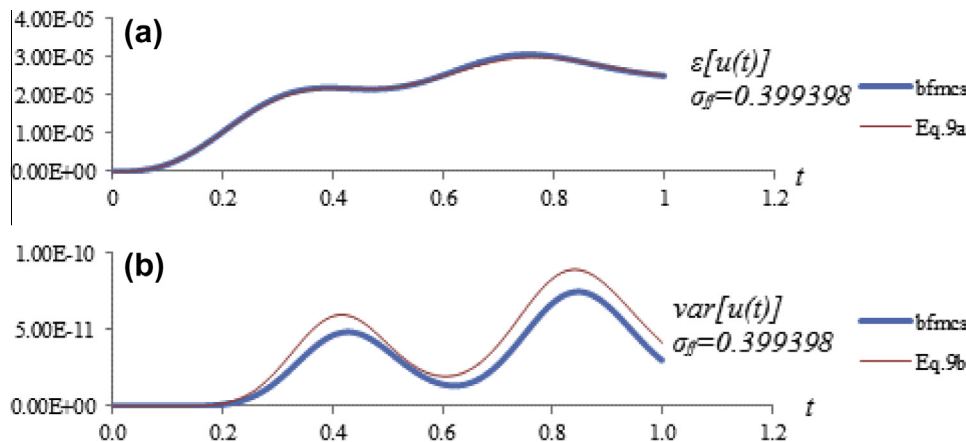


Fig. 8. Time histories of the (a) mean and (b) variance response displacement of the frame structure for a lognormal field with $\sigma_{ff} = 0.399398$ for LC1. Comparison of results obtained from Eq. (9a) and (9b) and MCS.

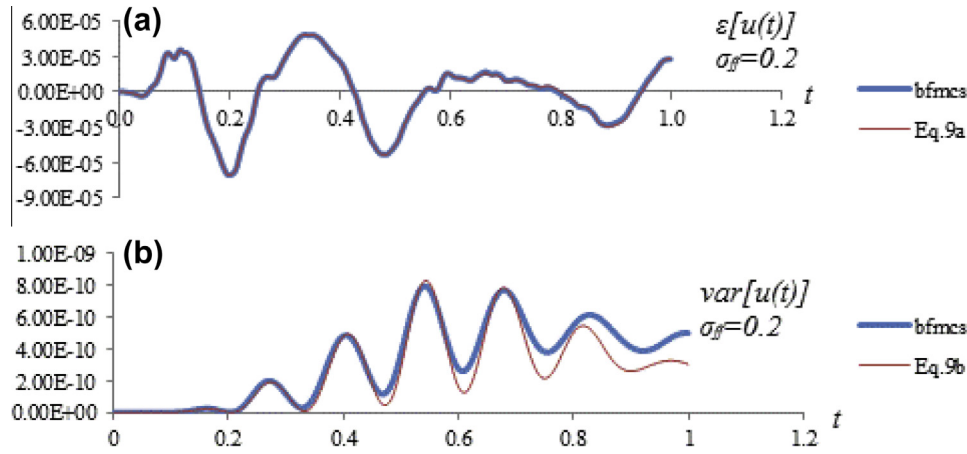


Fig. 9. Time histories of the (a) mean and (b) variance response displacement of the frame structure for a Gaussian field with $\sigma_{ff} = 0.2$ for LC2. Comparison of results obtained from Eqs. (9a) and (9b) and MCS.

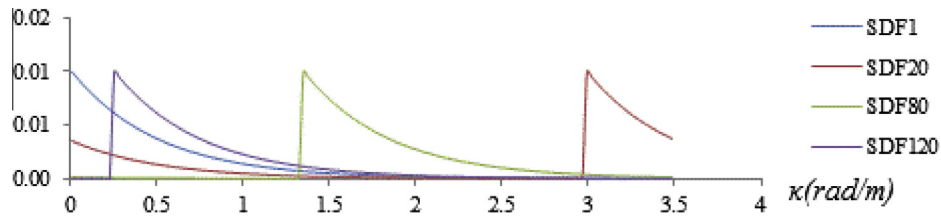


Fig. 10. Plots of different spectral density functions of the S_p family for a discretization of 128 steps in the frequency domain.

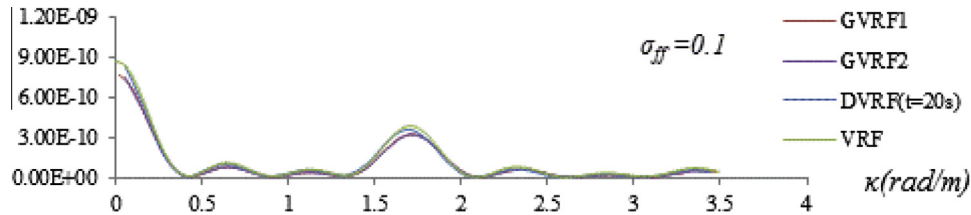


Fig. 11. Plots of $DVRF(u_A, t = 20 \text{ s})$ for a constant load, $GVRF1$ and $GVRF2$ for truncated Gaussian and Log-normal stochastic fields respectively and static VRF as a function of frequency κ (rad/m) for $\sigma_{ff} = 0.1$ for the fixed-fixed frame in Fig. 1.

$$S_p(\kappa) = \sigma_{ff}^2 \exp(-2|\kappa|) \quad (25)$$

In each row of Eq. (21) corresponds a different SDF of the S_p family. After computing respective $SDFs$ for the truncated Gaussian and Log-normal fields as in previous from Eq. (24) the i th SDF in the i th row of Eq. (21) is defined as follows

$$S_{p_i}(\kappa) = \begin{cases} S_p(\kappa + \kappa_u - i\Delta\kappa + \Delta\kappa), & 0 \leq \kappa \leq (i - 1)\Delta\kappa \\ S_p(\kappa - i\Delta\kappa), & i\Delta\kappa \leq \kappa \leq \kappa_u \end{cases} \quad (26)$$

Four different $SDFs$ of the S_p family are depicted in Fig. 11. It is expected *a priori* that the dynamic response displacement of the system, when the applied load is constant through time, $P(t) = P_0$, and as soon as the system reaches a stationary state (theoretically as time t tends to infinity), will match the response of the system for the static case $u(t) = P_0/k$. Respectively, $DVRF(u_A)$ should also follow the $GVRF(u_A)$ curve as it is deduced by Eq. (9a) and [26]. Observing Fig. 10, it can be seen that the trend of both $GVRF_1$ for the Gaussian and $GVRF_2$ for the Log-normal field is captured efficiently from the $DVRF(u_A)$ curve at time $t = 20 \text{ s}$. All three curves also match the respective static $VRF(u_A)$ curve. Noted be that VRF , as well as

$DVRF$ curves, are essentially computed following the same methodology as in $GVRF$ where S_p is the delta function with concentrated power equal to σ_{ff}^2 at each wavenumber κ and the u -beta function being the respective marginal pdf . Also the Gaussian and Log-normal $GVRF$ curves are, as expected, practically identical.

Finally, the $GDVRF$ was computed for the fixed-fixed frame of Fig. 1 and LC1 for a time window $[0-0.2 \text{ s}]$ and a relatively large coefficient of variation $\sigma_{ff} = 0.5$. Fig. 12a and b present plots of this $GDVRF$ and the corresponding $DVRF$ computed with Eq. (9a). In addition Fig. 13 presents a snapshot of $GDVRF$ and $DVRF$ at $t = 0.2 \text{ s}$. From all Figures it can be observed that $GDVRF$ and $DVRF$ almost coincide.

Example 2 Consider now the shear wall in Fig. 14 with length and height equal to $L = 4 \text{ m}$, the inverse of the modulus of elasticity assumed to vary randomly within its surface according to Eq. (13) with $F_0 = (1.35 \times 10^8 \text{ kN/m})^{-1}$, $\nu = 0.2$, $t = 1.0$ and damping ratio $\zeta = 5\%$. The total mass of the beam is assumed to be $m_{tot} = 4000 \text{ kg}$, distributed evenly among the finite element nodes of the model. The wall is discretized into a total of 100 plain stress elements, 121 nodes and 242 d.o.f.'s. In this example the 2D version DFEM-

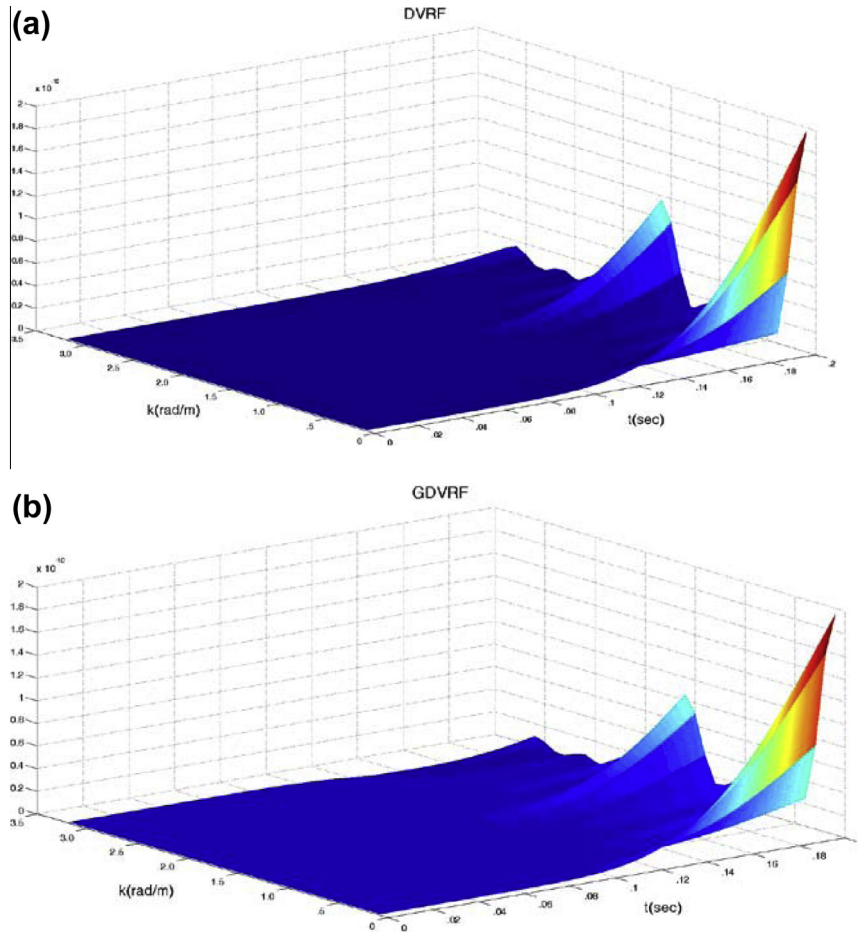


Fig. 12. 3D plots of (a) DVRF and (b) G DVRF of the horizontal displacement u_A , until $t = 0.2$ s as a function of frequency κ (rad/m) and time t (s) for LC1 and $\sigma_{ff} = 0.5$ for the fixed–fixed frame in Fig. 1.

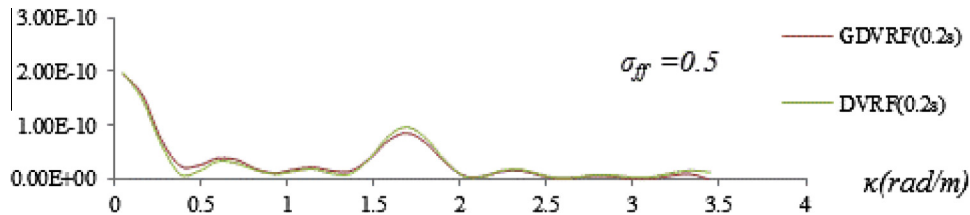


Fig. 13. Plots of $GDVRF(u_A, t = 0.2$ s) for LC1 and DVRF as a function of frequency κ (rad/m) for $\sigma_{ff} = 0.5$ for the fixed–fixed frame in Fig. 1.

FMCS procedure has been implemented, using Eq. (14) for the estimation of the dynamic mean and variability.

The same two load cases as in previous example are considered. The concentrated load is applied as shown in Fig. 3. In this example the following 2D spectrum has been implemented:

$$S_{f_{of_0}}(\kappa_x, \kappa_y) = \frac{\sigma_{ff}^2}{4\pi} b_x b_y \exp \left[-\frac{1}{4} (b_x^2 \kappa_x^2 + b_y^2 \kappa_y^2) \right] \quad (27)$$

where $b_x = 2.0$, $b_y = 4.0$.

Fig. 15 presents 3D plots of the $DMRF(u_A)$ and $DVRF(u_A)$ for the horizontal u_A displacement of point A of the shear wall as a function of frequency κ_x and κ_y for $\sigma_{ff} = 0.2$ at the fixed time of $t = 0.5$ s. It is observed that both $DMRF(u_A)$ and $DVRF(u_A)$ vary substantially with respect to both directions and as usual maximum

values are located at the vicinity of (0,0). Such plots can be drawn for all time steps of the analysis for the specific response displacement. Would one care to deduce realizable upper and lower bounds for this case, the extremes for $DMRF(u_A)$ ($DVRF(u_A)$) at each time step, accruing from the appropriate (κ_x, κ_y) pairs, should be selected and, after using Eq. (18), the bounds could be readily calculated. An application of the aforementioned procedure is shown in Fig. 16 for $\sigma_{ff} = 0.1$.

In following Figs. 17–21, results of mean and variability response are presented obtained from the DFEM-FMCS procedure and Eq. (14) in comparison with results obtained from Brute Force Monte Carlo Simulation. In Fig. 17, charts depict the comparison for the dynamic mean and variability response of the shear wall horizontal displacement at point A and LC1 for a Gaussian stochastic field with $\sigma_{ff} = 0.1$. In Fig. 18 respective results are presented for

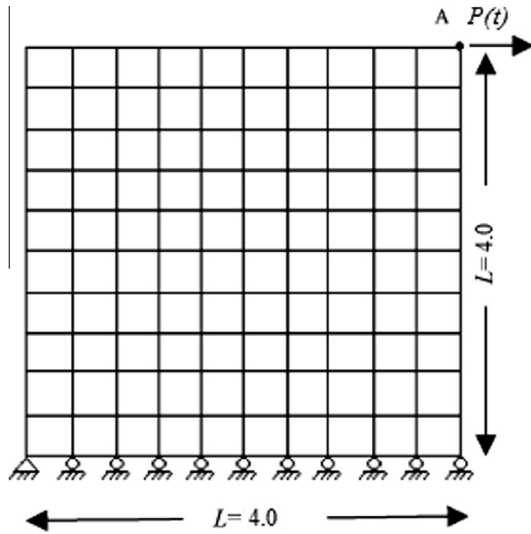


Fig. 14. Geometry, loading and finite element mesh of the shear wall.

a Gaussian stochastic field of $\sigma_{ff} = 0.2$. In Figs. 19 and 20 the results are respectively for a truncated Gaussian field with $\sigma_{gg} = 0.4$ and $\sigma_{gg} = 0.6$, respectively. The predictions of Eq. (14) in these cases

are very satisfactory with errors ranging up to 5–8%. At last, in Fig. 21 results of the mean and variability response for the shear wall and for LC2 are displayed for a lognormal stochastic field with $\sigma_{ff} = 0.2$. Again, the trend of the response is very well captured by Eq. (14) with errors ranging up to 15–20% in comparison to MCS.

7. Concluding remarks

In the present work, Dynamic Variability Response Functions and Dynamic Mean Response Functions are obtained for general stochastic FE systems such as a statically indeterminate frame structure and a plane stress shear wall problem with random material properties under dynamic excitation. The inverse of the modulus of elasticity was considered as the uncertain system parameter.

The DVRF and DMRF provide with an insight of the dynamic system sensitivity to the stochastic parameters and the mechanisms controlling the response mean and variability and their evolution in time. The recently established GVRF concept has been utilized and effectively validated the independence of DVRF of the spectral properties and the marginal pdf of the uncertain system parameter for the steady state loading case. Thus an easily implemented methodology is introduced for computationally efficient sensitivity analysis of general finite element systems.

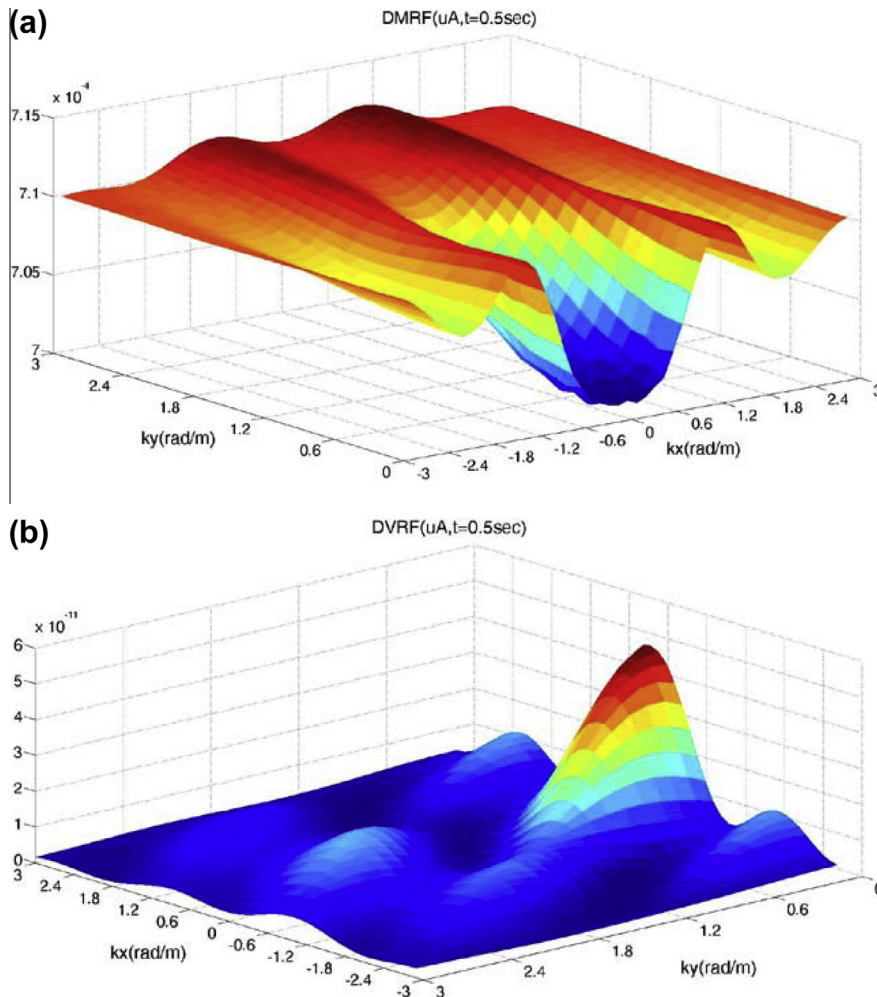


Fig. 15. 3D plots of (a) DMRF and (b) DVRF of the horizontal displacement u_A , at time instance $t = 0.5$ s as a function of frequency κ_x (rad/m) and frequency κ_y (rad/m) for LC1 and $\sigma_{ff} = 0.2$.

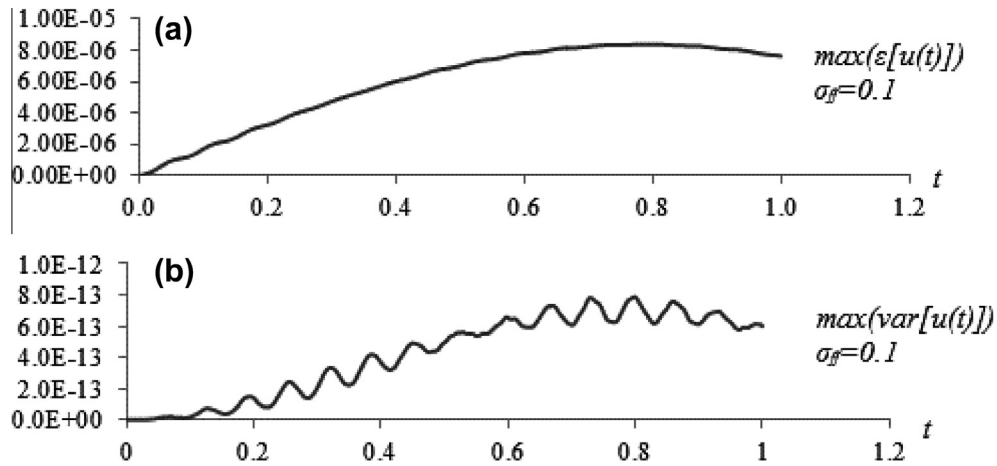


Fig. 16. Time histories of the (a) mean and (b) variance response displacement upper bounds of the shear wall for a Gaussian field with $\sigma_{\beta} = 0.1$ for LC1. Results obtained from Eqs. (12a) and (12b).

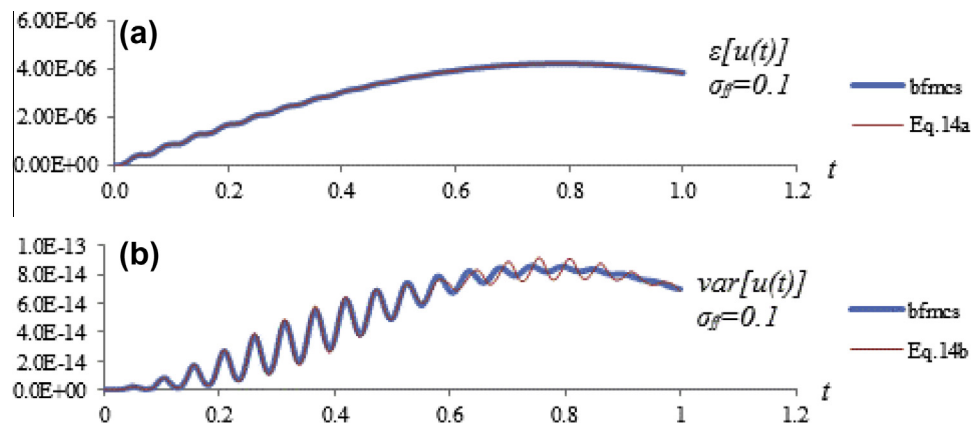


Fig. 17. Time histories of the (a) mean and (b) variance response displacement of the shear wall for a Gaussian field with $\sigma_{\beta} = 0.1$ for LC1. Comparison of results obtained from Eqs. (14a) and (14b) and MCS.

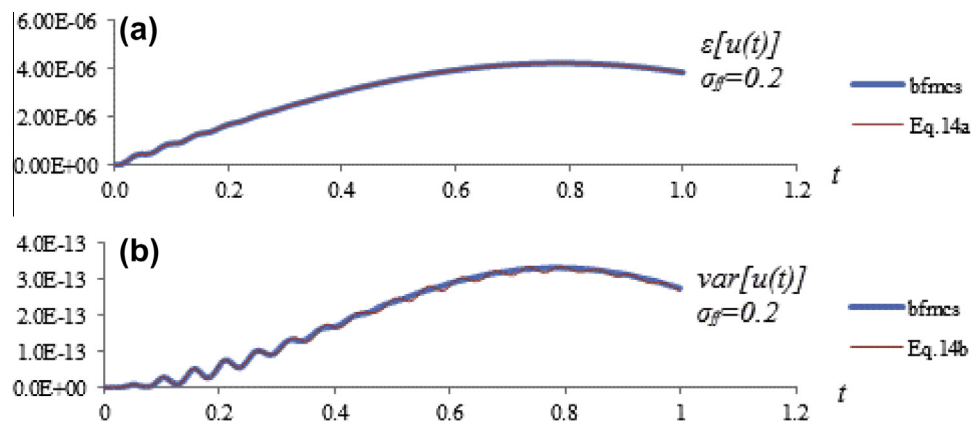


Fig. 18. Time histories of the (a) mean and (b) variance response displacement of the shear wall for a Gaussian field with $\sigma_{\beta} = 0.2$ for LC1. Comparison of results obtained from Eqs. (14a) and (14b) and MCS.

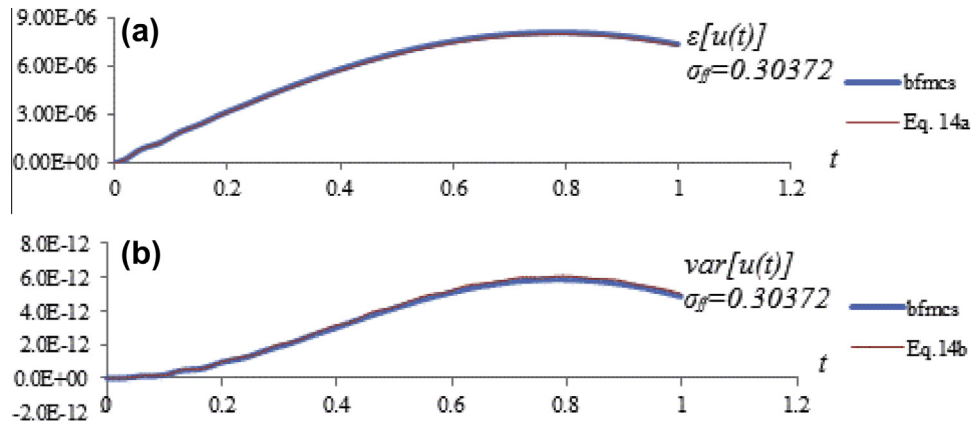


Fig. 19. Time histories of the (a) mean and (b) variance response displacement of the shear wall for an underlying Gaussian field with $\sigma_{gg} = 0.4$ for LC1. Comparison of results obtained from Eqs. (14a) and (14b) and MCS.

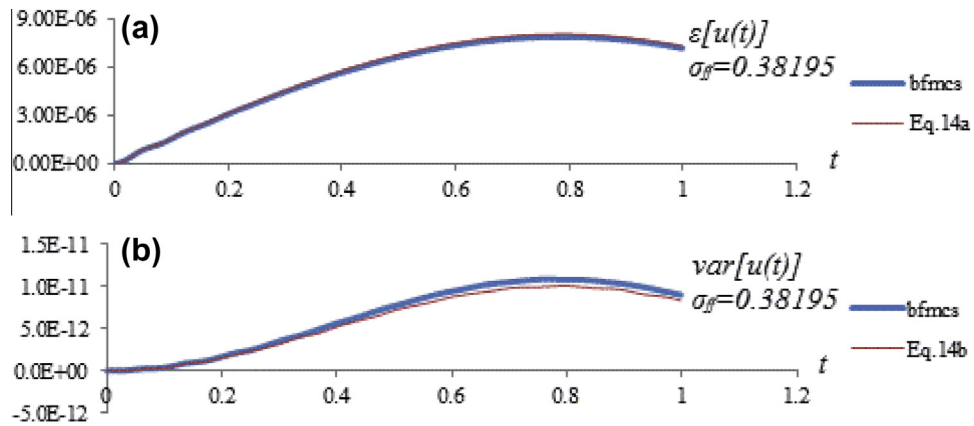


Fig. 20. Time histories of the (a) mean and (b) variance response displacement of the shear wall for an underlying Gaussian field with $\sigma_{gg} = 0.6$ for LC1. Comparison of results obtained from Eqs. (14a) and (14b) and MCS.

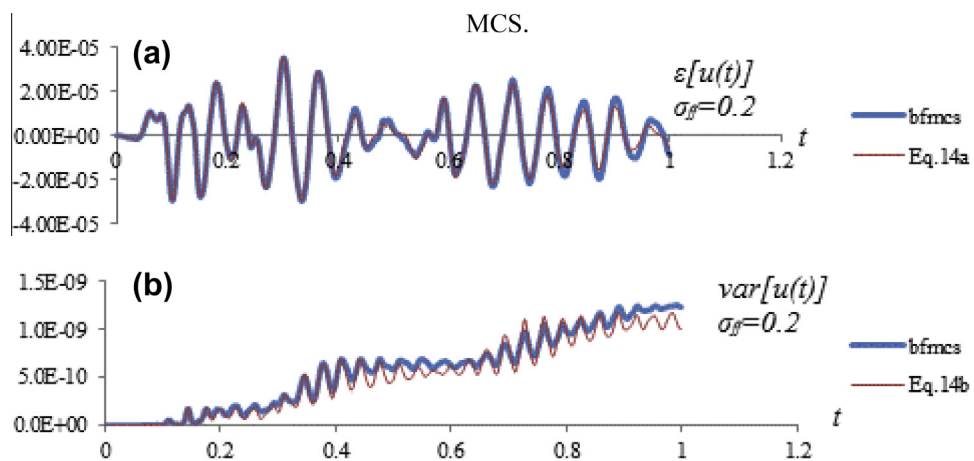


Fig. 21. Time histories of the (a) mean and (b) variance response displacement of the shear wall for a lognormal field with $\sigma_{gg} = 0.2$ for LC2. Comparison of results obtained from Eqs. (14a) and (14b) and MCS.

Acknowledgements

This work has been supported by the European Research Council Advanced Grant MASTER Mastering the computational challenges in numerical modeling and optimum design of CNT reinforced composites (ERC-2011-ADG-20110209).

References

- [1] Liu WK, Belytschko T, Mani A. Probabilistic finite elements for nonlinear structural dynamics. *Comput Meth Appl Mech Eng*. 1986;56:61–86.
- [2] Liu WK, Belytschko T, Mani A. Random field finite elements. *Int J Numer Meth Eng* 1986;23:1831–45.
- [3] Ghanem R, Spanos PD. *Stochastic finite elements: a spectral approach*, Springer-Verlag, Berlin (1991). 2nd ed. NY: Dover Publications; 2003.
- [4] Grigoriu M. Evaluation of Karhunen-Loève, spectral and sampling representations for stochastic processes. *J Eng Mech (ASCE)* 2006;132:179–89.
- [5] Matthies HG, Brenner CE, Bucher CG, Guedes C. Soares, Uncertainties in probabilistic numerical analysis of structures and solids – stochastic finite elements. *Struct Saf* 1997;19:283–336.
- [6] Stefanou George. The stochastic finite element method: past, present and future. *Comput Methods Appl Mech Eng* 2009;198(9–12):1031–51.
- [7] Zhao L, Chen Q. Neumann dynamic stochastic finite element method of vibration for structures with stochastic parameters to random excitation. *Comput Struct* 2000;77:651–7.
- [8] Liu WK, Besterfield G, Belytschko T. Transient probabilistic systems. *Comput Meth Appl Mech Eng* 1988;67(1):27–54.
- [9] Ghanem R, Spanos PD. Polynomial chaos in stochastic finite elements. *J Appl Mech* 1990;57:197–202.
- [10] Jensen H, Iwan WD. Response of systems with uncertain parameters to stochastic excitation. *J Eng Mech* 1992;118(5):1012–25.
- [11] Li J. The expanded order system method of combined random vibration analysis (in Chinese). *Acta Mech Sin* 1996;28(1):66–75.
- [12] Li J, Liao ST. Response analysis of stochastic parameter structures under non-stationary random excitation. *Comput Mech* 2001;27(1):61–8.
- [13] Yamazaki F, Shinozuka M, Dasgupta G. Neumann expansion for stochastic finite element analysis. *Eng Mech* 1988;114(8):1335–54.
- [14] Papadrakakis M, Papadopoulos V. Robust and efficient solution techniques for the stochastic finite element analysis of space frames. *Comput Methods Appl Mech Eng* 1996;134:325–40.
- [15] Papadrakakis M, Kotsopoulos A. Parallel solutions methods for stochastic FEA using Monte Carlo Simulation. *Comput Meth Appl Mech Eng* 1999;168:305–20.
- [16] Li J, Chen JB. The probability density evolution method for dynamic response analysis of non-linear stochastic structures. *Int J Numer Meth Eng* 2006;65:882–903.
- [17] Li J, Chen JB. Probability density evolution method for dynamic response analysis of structures with uncertain parameters. *Comput Mech* 2004;34:400–9.
- [18] Kougioumtzoglou IA, Spanos PD. An analytical Wiener path integral technique for non-stationary response determination of nonlinear oscillators. *Probab Eng Mech* 2012;28:125–31.
- [19] Ghosh D, Ghanem R, Red-Horse J. Analysis of eigenvalues and modal interaction of stochastic systems. *AIAA J* 2005;43(10):2196–201.
- [20] Schueller GI. Model reduction and uncertainties in structural dynamics. In: Papadrakakis M, Stefanou G, Papadopoulos V, editors. *Computational methods in stochastic dynamics*. Springer; 2011.
- [21] Papadopoulos V, Kokkinos O. Variability response functions for stochastic systems under dynamic excitations. *Probab Eng Mech* 2012;28:176–84.
- [22] Shinozuka M. Structural response variability. *J Eng Mech* 1987;113(6):825–42.
- [23] Wall FJ, Deodatis G. Variability response functions of stochastic plane stress/strain problems. *J Eng Mech* 1994;120(9):1963–82.
- [24] Graham L, Deodatis G. Weighted integral method and variability response functions for stochastic plate bending problems. *Struct Saf* 1998;20:167–88.
- [25] Papadopoulos V, Deodatis G. Response variability of stochastic frame structures using evolutionary field theory. *Comput Meth Appl Mech Eng* 2006;195(9–12):1050–74.
- [26] Miranda M, Deodatis G. Generalized variability response functions for beam structures with stochastic parameters. *J Eng Mech* 2012;138(9):1165–85.
- [27] Teferra K, Deodatis G. Variability response functions for beams with nonlinear constitutive laws. *Probab Eng Mech* 2012;29:139–48.
- [28] Papadopoulos V, Papadrakakis M, Deodatis G. Analysis of mean response and response variability of stochastic finite element systems. *Comput Meth Appl Mech Eng* 2006;195(41–43):5454–71.
- [29] Papadopoulos V, Deodatis G, Papadrakakis M. Flexibility-based upper bounds on the response variability of simple beams. *Comput Meth Appl Mech Eng* 2005;194 (12–16)8;1385–404.
- [30] Shinozuka M, Deodatis G. Simulation of stochastic processes by spectral representation. *Appl Mech Rev* 1991;44(4):191–203.
- [31] Grigoriu M. *Applied non-gaussian processes: examples, theory, simulation, linear random vibration, and MATLAB solutions*, Prentice Hall, 1995.